Journal of
Marine Science and Engineering

MDPI

Article

A Submersible Power Station: Part A Helium Power Conversion Unit

Jon Serna [1], Eduardo Anselmi Palma [2], Stefania Romero [2], Dimitrios Fouflias [1,*] and Pericles Pilidis [1]

[1] Thermal Power & Propulsion, Cranfield University, Bedford MK43 0AL, UK; p.pilidis@cranfield.ac.uk (P.P.)
[2] School of Aerospace, Transport & Manufacturing, Cranfield University, Bedford MK43 0AL, UK; e.a.anselmipalma@cranfield.ac.uk (E.A.P.); s.m.romerorenteria@cranfield.ac.uk (S.R.)
* Correspondence: dimi.f250@gmail.com; Tel.: +44-30-6984076018

Abstract: Nuclear power continues to hold great promise in the green revolution, however public opinion regarding its deployment is mixed. A submersible nuclear power station concept is presented here that is expected to allay many concerns that are holding back the growth of nuclear power. This submersible can move under its own power during emergencies and routine maintenance. Being stationed at sea it is earthquake proof. In the case of a tsunami it could decouple from the coast and sail to a location several miles to deeper waters in less than 30 min. Furthermore, it could be built, commissioned, maintained, refueled and scrapped in a country like the UK. This makes it proliferation-proof, a key concern with the wider deployment of nuclear power. In the present evaluation the philosophy and the electric power generation capability of the submersible power station are investigated. This includes a pre-feasibility visualization of the design. An evaluation is carried out into fitting it in a submersible of a size similar to the largest existing nuclear submarines. These designs may enable it to deliver 0.6 to 1 GW of electrical power.

Keywords: nuclear for energy applications; vessel; electric; power; propulsion

Citation: Serna, J.; Anselmi Palma, E.; Romero, S.; Fouflias, D.; Pilidis, P. A Submersible Power Station: Part A Helium Power Conversion Unit. *J. Mar. Sci. Eng.* **2024**, *12*, 2101. https://doi.org/10.3390/jmse12112101

Academic Editors: Paulius Rapalis and Sergejus Lebedevas

Received: 4 October 2024
Revised: 10 November 2024
Accepted: 13 November 2024
Published: 19 November 2024

1. Introduction

Increased electrification is bringing heightened concern regarding emissions [1]. Nuclear power is seen as a source of electricity that does not result in direct carbon emissions. The nuclear power life-cycle carbon footprint is comparable to the emission values expected for many renewable sources [2]. The low carbon footprint and the high utilization of the plant makes this type of energy an attractive alternative to partly replace fossil fuel power plants based in combustion processes [3,4].

There are significant pressures that are expected to increase electricity demand; many of these related to the legal requirement to reduce carbon dioxide emissions. Electric vehicle consumption will expand rapidly as government combustion vehicle restriction policies are applied [5]. Taking into account the average car sale numbers per year and the increasing penetration of electric cars, 7.24 million new electric vehicles are expected to be registered between 2030 to 2050. This would greatly increase electricity demand. Furthermore hydrogen, seen as a central vehicle for decarbonization [6] will be produced in vast quantities requiring electricity for the electrolysis of water.

On a more holistic basis, a quadrupling of electricity supply has been evaluated [7] for the UK to decarbonize its economy. In the same evaluation, a more than quadrupling of the generating capacity is predicted if based on renewables, while less than double the capacity is needed if this electricity is supplied through plant that can offer continuous operation like nuclear power. Other benefits of nuclear power include the delivery of a source of high grade heat and the modest footprint of the equipment.

However, nuclear power generates a social concern, primarily, due to three large nuclear accidents. These are the Three Mile Island PWR, the Chernobyl RBMK nuclear reactor [8] and the Fukushima Daiichi PWR reactors disaster [9]. The Pacific Ocean is

very prone to earthquakes and tsunamis. Tsunamis appear as an energy transmission phenomena from tectonic plate's movement. Tectonic plate's movement generates strain to the upper plate by friction compression. When this large amount of energy is released, it is transferred to the surrounding water emitting waves able to travel up to 800 km/h [10]. In deep waters, tsunamis are difficult to detect due to its low wave height.

The focus of this study is primarily on the power conversion unit and how to fit in the envelope of a new hull based on the main dimensions of an existing large submarine, noting that this will be a new submersible and not a retrofit. In the present study the authors, in this first attempt, adhered to the primary envelope size of the existing submersible, where the public information available was used as an input for the analysis. This may need to be modified once a second step is carried out on a more detailed analysis of the reactor at the core of the concept. Reactor shape and size constraints are recognised and not dealt in detail here. This is allowed for by including a conning tower with a height that is not specified. Extensive additional analysis will be needed on the assessment of the reactor shape and size and the redesign of the submersible shape to accommodate operational and safety requirements. There is some flexibility in slightly altering the shape of the envelope of the submersible, considering that a maximum operating depth of 70–100 m will be adequate. The original test depth of the Typhoon-class was a much deeper 400 m [11]. This large reduction of operating submerged depth and pressure will significantly reduce the constraints on hull design and permit alternative shapes in the vicinity of the reactors to accommodate their requirements. The authors consider the results described here as a useful contribution and as an encouragement to progress to the next stage, and refining the details of the concept.

2. Philosophical Basis of the Concept Proposed

The original inspiration for the submersible nuclear power plant arose from observations associated with the Fukushima accident. Nearly one hour of warning was available between the earthquake and the time it took for the tsunami to reach the coast. If in these 40–50 min a submersible power station could be decoupled quickly from the grid to travel a few miles off-shore and submerge a few tens of meters in deeper water, it should be able to survive the tsunami comfortably. Furthermore, such a power plant would be immune to earthquakes. With the very high power available on board, it should be able to sail swiftly from one location to another in the case of an emergency. In this context it could also be designed with a high cruise speed to reduce transit times and enhance return on capital.

It could very quickly be realised that such a power plant would also offer another very significant advantage. It would be much more protected from the concern of proliferation. The hypothesis was extended to envisage a production base or shipyard in the UK. This site would also be the location where all the refueling activities would take place. Any maintenance and the final decommissioning would also take place in this base. So, the submersible power station would be constructed and commissioned at this base, it would then travel to, possibly, very distant locations to produce electricity. When refueling or any maintenance is needed, the power station would return to the UK for these purposes and a replacement would be sent to produce electricity in the location of the demand. When the submersible power station reaches the end of its life it would return to this base to be decommissioned and scrapped. Thus any handling, processing and storage would take place in the UK protecting the power station from proliferation risks.

At this stage the costs have not been evaluated. There are factors that are expected to put an upward pressure on costs, such as the submersible hull, navigation and propulsion plant. However, there are expected to be many and significant factors that would bring cost benefits. For example, there would be no purchases of land needed, and the frequent planning obstacles, delays and costs associated with the identification of a suitable land site. It would be more distant form the population at large if it was located, for generation purposes, a handful of km offshore. Plant cooling would be readily available. Site preparation would not be needed other than the electrical connections and switchgear and equipment

to connect and disconnect from the grid. The construction teams and equipment (some of it heavy) need not move from one location to another as all the power stations would be constructed one after the other on the same location. The same would apply to refuelling processes and fuel transport. This approach would enable many power plants of the same design to be produced accruing economies of scale for both the design and the construction processes. On balance it is likely that, for a large production batch of submersibles, the costs may be similar to that of a shore based power station, with the added benefits of earthquake and tsunami protection plus much lower anti proliferation risks.

3. Research Scope—Objectives

The present study focuses in the preliminary selection and calculation of the principal thermodynamic and mechanical systems of the submergible power plant, as well as the overall component integration in the submergible vessel in order to prove it's feasibility. Initially, the reactor type was selected based on previously implemented vessel reactors. This implies a compact and modular design able to deliver a power output comparable to a land-based power plant but with space restrictions. The reactor design details are not explored here but a realistic allowance for its size is made in the submersible envelope. Once a feasible reactor type, total plant power output and number of reactors was selected, different thermodynamic cycle configurations were analysed. Plant thermal efficiency and overall power output were calculated and compared between different configurations. Heat and mass balance analysis were carried out, excluding turbomachinery, heat exchanger and piping designs, as well as electrical installation and control systems. In order to determine the size of the submersible vessel, reactor size and helium working turbomachinery sizes were calculated. Vessel auxiliary systems such as reactor shutdown process, including RHR system, and vessel propulsion system were designed.

Intercooled-regenerated Brayton cycles have been considered here as they can deliver high efficiency. This study compared the performance, specific power output and thermal efficiency of intercooled-recuperated Brayton cycles with a combined-cycle gas turbine configuration. Based on the possible location of the power plant and helium cooled reactor and turbomachinery limitations, design basis key cycle input parameters were modified to maximize the performance and reduce the volume to power output ratio of the selected cycle.

4. Helium Thermodynamic Cycle Analysis

Helium offers useful thermodynamic and chemical characteristics that make possible the downsizing of future nuclear power plants. It offers higher heat transfer capabilities enabling a more compact heat exchanger design for pre-coolers, intercoolers, regenerators and HRSGs. Helium would be operated in a Brayton closed cycle, which reduces turbomachinery fouling compared to open cycle gas turbines. The closed cycle permits much higher minimum pressures and resulting in smaller size turbomachinery. Regarding the helium turbomachinery design considerations, the drop in polytropic efficiency due to the Reynolds number effect is slightly reduced from 0.9% to 0.2% approximately compared to air. Helium's higher velocity of sound also appears as an advantage for the turbomachinery design process as it allows higher peripheral speeds before the onset of Mach Number effects. Helium's low molecular weight would result in an increased number of turbomachinery stages, however, the higher peripheral speeds that could be achieved would counteract the negative effect of low molecular weight [12].

4.1. Helium Thermodynamic Cycle General Methodology

The thermodynamic cycle general development methodology was based in a feasibility and general optimisation iteration process. The flow chart defining the methodology implemented is shown in Figure 1. Determining the performance of a thermodynamic cycle implies assuming inputs according to a certain criteria. The objective of this analysis is to obtain the thermal efficiency and specific power output of both analysed cycles for a

further performance comparison and final selection. Moreover, these results were obtained for a range of overall pressure ratios and therefore, a design point selection was carried out.

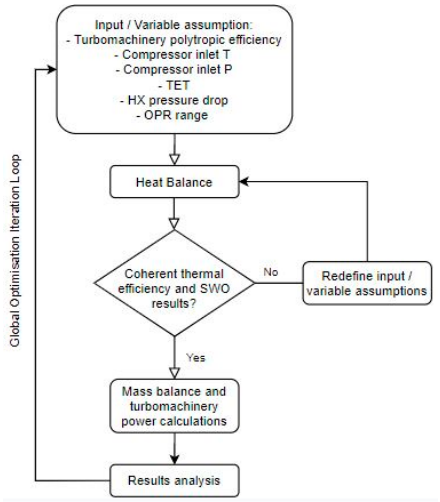

Figure 1. Helium thermodynamic cycle methodology flow chart.

Defining the compressor inlet temperature T1 (290 K) relies on the pre-cooler cooling water temperature selection. This temperature was selected taking into consideration the ocean surface mean temperature (16 °C). This selection affects directly the thermal efficiency of the cycle, obtaining higher efficiency values by lowering the compressor inlet temperature. World´s ocean temperature distribution was considered as a guide for future power plant location selection [13]. Being a close cycle, the compressor inlet pressure P1 (1000 kPa) may be varied to reduce the required piping and turbomachinery size. By increasing P1, the working fluid density also rises affecting significantly the required piping and turbomachinery casing wall thickness and hence, the machinery weight will vary.

The turbine entry temperature (1100 K) is restricted by the maximum metal temperature of the reactor vessel. Nevertheless, higher TETs will result in a higher overall cycle thermal efficiency, noting that the blades and the heat exchangers will not be cooled. In the present study a polytropic efficiency (ηpoly) of 0.9 was adopted for helium turbomachinery. This is inspired from helium turbomachinery for a GT-MHR power plant that reports polytropic efficiencies between 0.88–0.9 for the compressor and up to 0.93 for the turbines [14].

Regarding pressure losses in heat exchangers, conservative criteria were applied by selecting 2.5% of pressure loss, considering average pressure losses between 1% and 2% for heat exchangers working with gases. The HRSG efficiency value (ηHRSG) of 0.97 was selected as the only heat losses happening in this closed heat exchanger have their origin in convection and radiation. Steam turbine inlet $P_{1'}$ was 7000 kPa, Steam turbine discharge $P_{2'}$ was 3 kPa and Steam turbine isentropic efficiency (η_{ST}) 0.85.

4.2. Cycle Comparison and Selection

Helium nuclear concepts have been traditionally considered with intercooled, reheated and recuperated Brayton cycles. In order to improve the performance of the power generation cycle, two thermodynamic cycles were analysed and compared according to thermal efficiency and specific work output. The optimised Brayton cycle (Figure 2) being an Intercooled, Recuperated and Reheated Brayton cycle (working fluid: Helium) was compared to a combined cycle (Figure 3) with Reheated Brayton (working fluids: Helium and Steam), considering CCGTs are able to offer higher thermal efficiencies than most optimised Rankine and Brayton cycles.

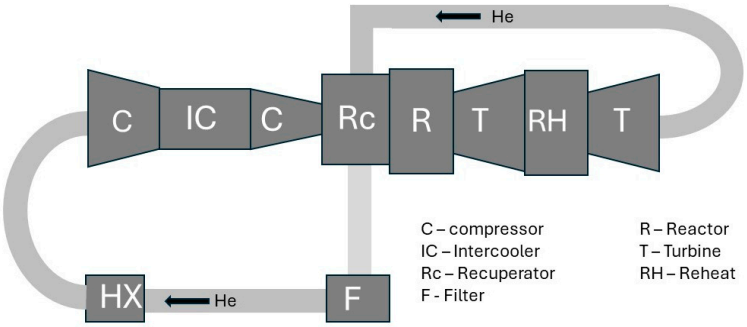

Figure 2. Helium Intercooled, Recuperated and Reheated Brayton cycle flow diagram.

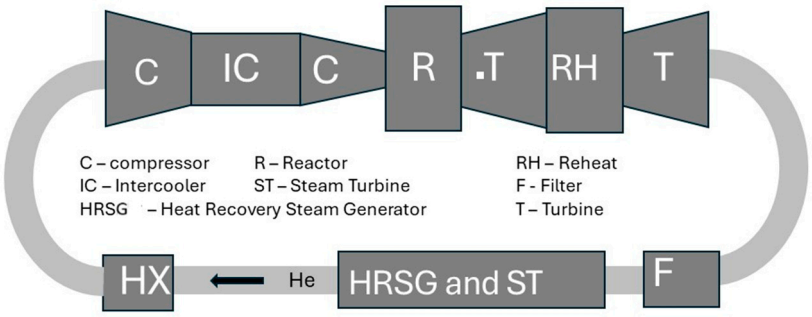

Figure 3. Combined cycle (Reheated Brayton) flow diagram.

A heat balance was carried out for both cycles in order to determine the thermal efficiency and specific work output. Mass balance was also carried out for each cycle with the objective of defining the mass flow required for 3 total electric power outputs (150MW(E), 200MW(E) and 250MW(E) per reactor). For the intercooled, reheated and recuperated Brayton cycle an overall pressure ratio range between 2.89 and 6.76 was analysed. It was found that for the same overall PR, the best thermal efficiency was obtained by applying the same PR for both high and low pressure compressors. For the combined cycle an overall pressure ratio range between 4 and 14.44 was analysed. Pressure and temperatures for the Combined Cycle are shown in Table 1 (for the highest thermal efficiency pressure ratio design point).

Table 1. Combined Cycle Ts and Ps for each state.

OPR = 5.76	Temperature [K]	Pressure [kPa]
1—Compressor inlet	290	1000
2—Compressr outlet	428	5760
3—Turbine inlet	1100	5616
4—Turbine outlet	759	2000.84
5—PT inlet	1100	1950.82
6—PT outlet	881	1051.94
7—PC inlet	318	1025.64
1′—ST inlet	822	7000
2′—ST outlet (X = 0.8)	297	3
3′—Pump inlet	297	3
4′—HRSG inlet	297	7000

4.3. Brayton Cycle and Combined Cycle Performance

Considering the Brayton cycle, thermal efficiency and specific work output were obtained for an overall pressure ratio range from 2.89 to 6.76. Results are shown in Figure 4.

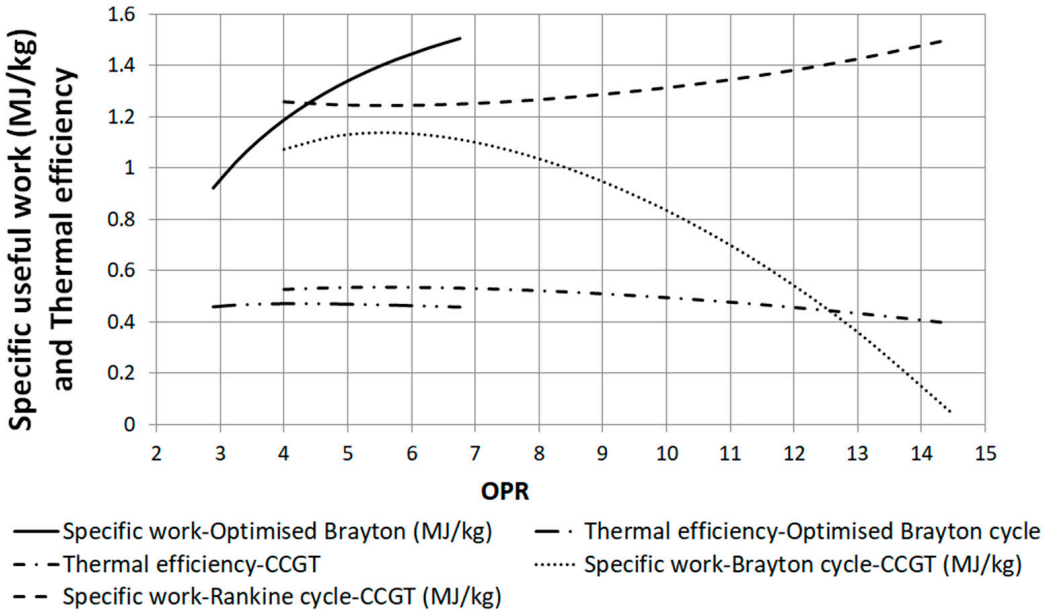

Figure 4. Optimised cycle versus Combined cycle performance.

A maximum thermal efficiency of 0.471 was obtained for an OPR of 4, whilst the specific work output continued to rise as the OPR was increasing. The specific work output value for the maximum thermal efficiency point was 1187.3 KJ/KgHe. Considering the combined cycle, thermal efficiency and specific work output were obtained for an overall pressure ratio range from 4 to 14.44. Maximum thermal efficiency value (53.54%) was obtained for an OPR of 5.76. Comparing Brayton cycle specific useful work to that related to Rankine it was observed that after a pressure ratio value of 5.76 the Rankine specific useful work increased quadratically while the Brayton cycle specific useful work followed an almost inversely proportional quadratic drop. This illustrated the Rankine cycle's superiority in terms of useful work after an overall pressure ratio level.

4.4. Mass Balance for a Range of Power Plant Electrical Power Outputs

The mass flow results obtained for 3 different power plant outputs ranging from 600MW(E) to 1GW(E) were investigated. Four reactors were considered in the design of the submersible, therefore, the total electrical power output per reactor would range from 150MW(E) to 250MW(E), shown in Table 2.

Table 2. Required mass flow and turbomachinery powers (Brayton).

OPR = 4	150 MW(E)	200 MW(E)	250 MW(E)
Mass flow $[kg_{He}/s]$	126.33	168.44	210.55
Turbo-comp power [MW]	137.05	182.74	228.42
PT power [MW]	150	200	250

For the purpose of calculating the required steam and helium mass flows for the combined cycle, a steam mass flow to helium mass flow ratio was defined (given value corresponds to the maximum thermal efficiency point, Table 3):

$$\frac{\dot{m}_{H_2O}}{\dot{m}_{He}} = \frac{\eta_{HRSG} \cdot Cp_{He} \cdot (T_8 - T_9)}{2526.08 + 1.996 \cdot (T_{1'} - 558.9)} = 0.9271 \quad (1)$$

Table 3. Required mass flow and turbomachinery powers (Combined cycle).

OPR = 5.76	150 MW(E)	200 MW(E)	250 MW(E)
Helium mass flow $\left[kg_{He}/s\right]$	65.5	87.33	109.16
Steam mass flow $\left[kg_{H20}/s\right]$	60.72	80.97	101.21
Turbo-comp power [MW]	115.94	154.58	193.22
Helium PT power [MW]	74.48	99.3	124.12
Steam PT power [MW]	75.52	100.7	125.88

4.5. Results Analysis 1

Higher thermal efficiencies for the CCGT cycle imply that for a certain reactor thermal output, higher electrical power output will be obtained. Reactor outlet coolant temperature (or TET) was selected considering a conservative approach. Even for this value of TET, the current study achieved better thermal efficiency values than intercooled, recuperated and reheated cycles analysed. However, applying state of the art TET values to the cycle could result in a cycle thermal efficiency of up to 3% more than the results obtained (for a TET of 950 °C achieved in reactors such as the AVR reactor or the HTTR reactor [15]), reaching values of up to 56.5%.

Although the Brayton intercooled, recuperated and reheated cycle could offer higher specific work output, it would only reduce the turbomachinery size without increasing the total electrical power output of the cycle, as the heat input is fixed by the maximum reactor size that could be implemented. Therefore, CCGT was selected as the most suitable thermodynamic cycle to be implemented coupled with a PBMR for a submersible nuclear power plant.

In order to improve the economic and environmental feasibility of the submersible power plant in long term, thermodynamic cycle analysis had been carried out improving the thermal efficiency compared to conventional cycles implemented with nuclear reactors. CCGT configuration was selected showing efficiencies above 53.5%. This increase would reduce both fissile fuel and radioactive waste management costs.

Regarding the integration of the reactors and turbomachinery inside the submersible vessel, a double internal pressure hull design was selected, providing space for a total of 4 reactor configuration with a total electrical power output of 1GW(E).

5. Power Plant Integration in a Double Pressure Hull Submarine Vessel

This section aims to offer a visualization of what such a submersible power station could look like. Many of the methods and evaluations include uncertainties and estimations, in particular those related to reactor shape and size. Nonetheless a useful approximate view of the concept is possible. This initial step or iteration is intended as a basis for subsequent refinements and improvements of the design concept. In this section an approximate sizing exercise is offered, noting that many uncertainties remain.

5.1. Typhoon-Class Submarine Generation, HTR Technology and State of the Art

The aim was to consider a new submersible utilizing the primary dimensions of the Typhoon-class, the largest submarine to be used. The concept presented here is a new arrangement able to fit the required machinery and propulsion systems under investigation analysed in the present study. Some technical specifications of a Typhoon-class submarine were obtained. This submarine featured a total length of 175 m, 23 m beam and 12 m draught. This beam length was necessary to fit the double main pressure hull design. The two main pressure hulls diameter was reduced towards the bow in order to fit 20 nuclear missiles [16].

The vessel water displacement is 23,500 water tons surfaced and 48,000 tons submerged. The submarine could also cruise through and under ice platforms, featuring an ice-breaking sail and sail-guards as well as retractable nose horizontal hydroplanes. This feature could improve the feasibility of a submersible power plant to reach remote populated areas where the electrical power is transported through thousands of kilometers.

The submarine featured a double Pressurized Water Reactor design installed inside the two main internal hulls, providing a thermal power output of 190 MW and it was paired to a steam turbine producing a shaft power of 37.5 MW per reactor. A total power of 75 MW was sent to two seven bladed propellers, providing a maximum cruise speed of 12 knots surfaced and 25 knots submerged. The propellers featured a ducted design [17] and the whole external hull was covered by sound absorbing tiles for silent operation.

5.2. ASME VIII Div. I Design Code for Pressure Vessels

The ASME VIII Div. I design code is based in the design of pressure vessels for internal and external pressure requirements. The vessels calculated according to this code are considered thin wall vessels and the mechanical stress perpendicular to the shell or vessel heads is considered zero. In this particular case, the calculated vessel was going to work under external pressure only. Division I of the code offers a conservative approach, calculating the thickness requirement according to the maximum normal stress theory. Division II of the code offers a more complex analysis of stresses, based on the maximum distortion energy theory (Von Misses). According to the vessel design pressure and diameter, ASME offers recommendations to select the Division [18] for better vessel design.

To design a vessel according to this code, all the minimum design safety factors and methodology had to be followed and the design conditions had to be defined according to the code criteria. Design temperature is defined as the temperature for which the selected material has the worst performance. ASME VIII code defines a minimum safety factor of 1.1 for design pressure selection for operating pressures above 300 psi. If the vessel operating pressure is below 300 psi, the design pressure value P_d would be defined as follows.

$$P_d = P_o + 30\text{psi} \tag{2}$$

Material selection was also carried out among a material list offered by the ASME VIII code. According to the design temperature selected, material yield strength and allowable stress was obtained. In order to calculate the thickness required for external pressure applications, the allowable pressure has to be calculated. Initially, shell length to vessel diameter ratio and vessel diameter to defined thickness ratio are obtained. Determining these two ratios, the value of "A" factor is obtained according to the ASME VIII code. According to this value and the design temperature, the value of "B" factor is obtained [18]. Once these two factors determined, the maximum allowable pressure P_a is defined as follows.

$$P_a = \frac{4B}{3 \cdot (D_o/t)} \tag{3}$$

If the allowable pressure value P_a exceeds the design pressure P_d, the obtained thickness for the vessel could be considered correct.

5.3. Radiation Shielding Sizing

Ionizing radiation emitted from radioactive reactions is the most important human threat. Gamma radiation is the strongest type, requiring the highest attenuation ratios to control the radiation levels for workers. In order to attenuate radiation levels outside the nuclear reactor area, shielding materials are implemented. The attenuation level depends mostly on the density of the material, showing higher attenuation levels for high density materials. The required shielding thickness depends on the mass absorption coefficient μ, the linear attenuation coefficient u and the attenuation ratio $\dot{X}/\dot{X}_o$. The mass absorption coefficient quantifies how easily electromagnetic radiation penetrates a material [19]. The linear attenuation coefficient is the product of mass absorption coefficient and the material density. The attenuation ratio is the ratio between the exposure rate after the reactor shielding has attenuated the radiation and the exposure rate in the proximities of the reactor. The expression to obtain the required shielding thickness for certain attenuation ratio is expressed by the reactor shielding equation as follows.

$$\dot{X} = \dot{X}_o \cdot e^{-u \cdot x} \quad (4)$$

Required reactor shield thickness calculation was carried out to determine the maximum reactor size that could be installed. The methodology was based on an iterative process in order to determine the most feasible material to be installed as the radioactive shield, taking into account space availability criteria in order to install the highest thermal output reactor possible. Reactor sizing is the biggest uncertainty of this study, in particular in the critical vertical dimension. To allow for this a conning tower of unspecified height is introduced in the design.

Nuclear Reactor Shielding Methodology

Required reactor shield thickness calculation was carried out to determine the maximum reactor size that could be installed (considering the assumptions made for the reactor sizing).

The methodology (Figure 5) was based on an iterative process in order to determine the most feasible material to be installed as the radioactive shield, taking into account space availability criteria so as to install the highest thermal output reactor possible and hence, improve the submersible power plant feasibility.

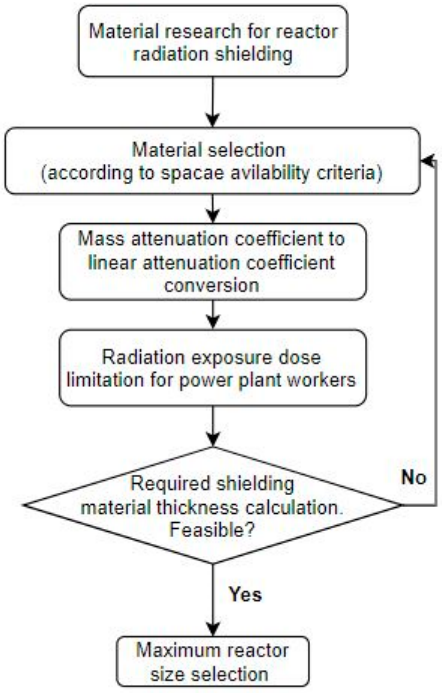

Figure 5. General methodology for reactor shield calculation.

5.4. Internal Pressure Hull Design

External pressure calculations require more iteration loops to optimise the material required thickness compared to internal pressure calculations for pressurized vessels. As shown in the flow chart of Figure 6, A and B factors must be calculated before checking the feasibility of a material thickness for certain input conditions. Once the allowable pressure surpasses the required one, the thickness must be reduced in following iteration loops until the SF of the ASME pressure requirement falls below 1.05.

The Typhoon-class internal hulls had a changing diameter design, with diameter values up to 10 m for the reactor and turbomachinery housing and they were designed for housing 2 reactors. The objective of the internal hull design of the current study was to optimise the overall internal hull design, from dimensions to material selection and required thickness. Design parameters were selected according to space availability

of the submersible power plant, packing most land-based nuclear plant features in a compact design and total power plant cost thus internal hull metal weight had to be kept minimum. The ratio between the operation and design pressures (Pressure Safety Factor) was selected to be 1.5, exceeding the minimum ASME VIII Div. I code safety factor of 1.1. So for 1500 kPa design pressure the operating pressure P had to be 1000 kPa which is representative for 100 m operation depth. Design temperature was defined at 50 °C, nearly the highest official temperature ever recorded at a value of 56.7 °C [20], verified by the World Meteorological Organization.

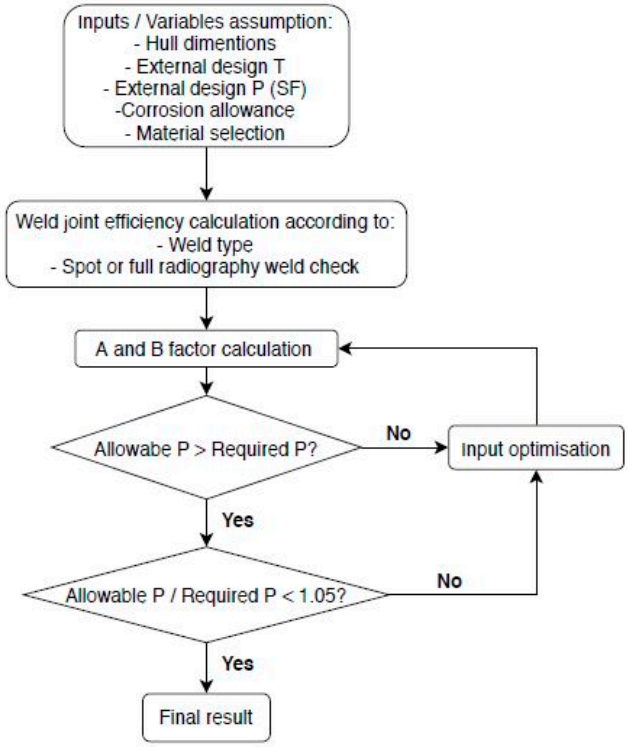

Figure 6. Internal pressure hull design general methodology.

Internal and external annual corrosion rates were defined under conservative criteria, considering the external corrosion rate (0.3 mm per year) has been selected for carbon steel operating with high corrosive fluids (saltwater) and internal corrosion rate (0.15 mm per year) has been set for medium corrosive fluids (high salinity concentration in air). Total values for corrosion allowance thickness, 8 mm for internal and 15 mm for external corrosion allowance have been defined for a 50 year nuclear plant operation life. Optimising the space availability of the submersible power plant, by removing all the nuclear ballistic missiles and the torpedo silo of the Typhoon-class submarine, the following dimensions could be reached as shown in Table 4.

Table 4. Internal hull dimensions.

Hull Dimensions	Value
Internal diameter Di [mm]	10,000
External diameter D_o [mm]	10,416
Height of heads (h) [mm]	2604
TL to TL length (TL) [mm]	117,000
Total shell length (L) [mm]	118,743

The Typhoon-class internal hulls were constructed of titanium, keeping the mechanical performance of steel at lower thicknesses but higher costs. In order to improve the cost feasibility of this project and taking into account that the maximum operation depth of the

submersible power plant in one quarter of the original vessel (400 m depth), the material employed for constructing the internal hulls would be a carbon steel, specifically the SA-516 Gr. 60 [21], widely used in the pressure vessel industry, with a modulus of elasticity (at design T) of 202,000 MPa, yield strength of 215 MPa and allowable stress of 118 MPa. The SA-516 Gr. 60 carbon steel composition is shown in Table 5:

Table 5. SA-516 Gr. 60 carbon steel composition [21].

Composition	Percentage	Composition	Percentage
C	0.18	Cu	0.3
Si	0.4	Ni	0.3
Mn	0.95/1.5	Mo	0.08
P	0.015	Nb	0.01
S	0.008	Ti	0.03
Al	0.02 (Min)	V	0.02
Cr	0.3		

Two internal pressure hull designs were considered at the present study. The original two-pressure hull design with constant internal diameter of 10 m and a four-pressure hull design should be required to withstand the same pressure value, as reducing the vessel total length increases its moment of inertia and requires less material, although the head thickness should remain the same, as it only depends on the internal and external head diameter ratio and the head geometry.

The required vessel thickness was only calculated for the constant diameter section, as reducing the hull diameter, while keeping the shell thickness constant, results in a higher moment of inertia than the constant diameter section and therefore, an increase of the safety factor. Also, the 4 pressure hull design reduces the TL to TL length to 56 m and the total length to 57.74 m. Head thickness values for both configurations were the same at 140 mm. The four pressure hull configuration showed a shell thickness of 200 mm which was 20 mm less compared to the two pressure hull configuration. However, the two hull design requires 4 heads whilst the four hull one requires 8. In order to find the configuration requiring less metal weight, calculations were carried out by determining the volume of both. The crown radius R, knuckle radius a and height h of a 2:1 Elliptical ASME VIII head were defined by Mueller pressure vessel manufacturer [22] as the 90% of the external diameter, 17% of the external diameter and one quarter of the external diameter respectively. Torispherical head volume calculation parameters [23] were taken into account and head volume calculations followed.

Quantifying the volume below the surface for the outer and internal diameter values, head metal volume V_{HEAD} was found to be 15.92 m^3. The total metal volume for the two pressure hull configuration was defined by the following expression (TL= 117 m).

$$V_{2HULL} = 4 \cdot V_{HEAD} + 2 \cdot \left[\left({R_o}^2 - {R_i}^2 \right) \cdot TL \right] = 1778 \ m^3 \quad (5)$$

The total metal volume for the four pressure hull configuration was defined by the expression as follows (TL = 56 m).

$$V_{4HULL} = 8 \cdot V_{HEAD} + 4 \cdot \left[\left({R_o}^2 - {R_i}^2 \right) \cdot TL \right] = 1621.5 \ m^3 \quad (6)$$

The weight saving in favor of the four pressure hull design was defined with the SA-516 Gr. 60 density.

$$W_{SAVING} = (V_{2HULL} - V_{4HULL}) * 7800 \frac{kg}{m^3} = 1220.4 \text{ tons} \quad (7)$$

Considering a saltwater density of 1029 Kg/m^3, the ballast tank volume saving was calculated (as a function of the internal hull weight saving) to be 1186 m^3.

$$V_{BALLAST\ TANK} = W_{SAVING}/\rho_{WATER} \quad (8)$$

5.5. Helium Turbomachinery Sizing Considerations

The sizing of helium turbomachinery attached to each PBMR was evaluated, concluding if the size required for the calculated plant power output is feasible considering the space available inside each internal pressure hull. Compared to air gas turbines, helium-working turbomachinery would result in a higher number of compression and expansion stages (for a given pressure ratio) due to the helium low molecular weight. Considering that helium specific heat is about five times that of air and that stage temperature rise is inversely proportional to the specific heat and directly proportional to the stage pressure rise, it can be concluded that helium would require more stages for the same pressure ratio [14]. However, closed cycles require less pressure ratio to reach the thermal efficiencies of open cycles, so less stages are required.

Closed cycle helium turbomachinery have small blade heights compared to air gas turbines resulting in high hub to tip ratios and low aspect ratios [14] and this is due to the fact that compressor inlet pressures are much higher than those adopted for open cycle gas turbines. Small blade heights imply higher end wall loses however, the loss in polytropic efficiency induced by this fact is compensated by low Mach numbers and oxide free blade surfaces (helium has no oxidizing agents). Also, blade cooling is not required for the specified TETs, as nickel-based alloys are able to work at 1100 K without melting or stress limitations. In order to evaluate the feasibility of the helium turbomachinery selected for the design point, turbo-compressor and power turbine power requirements were compared with the turbomachinery sizing study for a 286 MW(E) GT-MHR power plant [14]. CCGT turbomachinery power requirements are shown in Table 6.

Table 6. Power requirement for a range of CCGT electrical power outputs.

	150 MW(E)	**200 MW(E)**	**250 MW(E)**
Turbo-comp power [MW]	115.94	154.58	193.22
Helium PT power [MW]	74.48	99.3	124.12
Steam PT power [MW]	75.52	100.7	125.88

Taking into account that the highest power requirement of this study does not reach the 200 MW(E) and the maximum tip diameter for the 286 MW(E) turbo-compressor does not exceed 2 m, it can be stated that any of the considered helium turbomachinery could be installed in a 10 m diameter internal pressure hull, leaving the necessary space for auxiliary equipment.

To obtain a steam turbine diameter value for the intended application, GE's non-reheat GE STF-A100 steam turbine [24] was used as reference, considering that provides the turbine exhaust area value for a similar power output. An approximate exhaust area of 3.5 m^2 was given for 80MW(E) steam turbines, resulting in a steam turbine diameter around 2.2 m. Turbomachinery length was not a space restricting factor considering that each internal hull containing one reactor attached to its CCGT will have a total length of 55 m.

5.6. Reactor Sizing—Electrical and Thermal Power Outputs

The submarine total electrical power output relies on the maximum thermal power output that could be installed in a 10 m diameter internal hull. Considering that a four reactor plant design was selected and a total electrical power output range between 600MW(E) and 1GW(E) analysed, three reactor electrical power outputs were compared: 150MW(E), 200MW(E) and 250MW(E). According to the "High Temperature Gas-cooled Reactor Technology Training Curriculum" from Idaho National Laboratory [25], HTR thermal output per volume unit can vary in a range from 4MW(TH) to 6.5MW(TH). These values compared

to water cooled reactors offer a higher thermal power density, considering the space occupied by the reactor core and the coolant volume. A 4MW(TH) per effective volume cubic meter was selected. For the 600MW(E) power output nuclear power plant configuration (150MW(E)/reactor), the effective pressure vessel volume requirement was calculated.

$$Q = \frac{P_E}{\eta_{TH}} = \frac{150\ MW}{0.535} \approx 280\ MW(TH) \quad (9)$$

$$280\ MW(TH) \cdot \frac{1\ m^3}{4\ MW(TH)} = 70\ m^3 \quad (10)$$

For the 800 MW(E) power plant configuration (200 MW(E)/reactor), the effective pressure vessel volume requirement was calculated to be 93.75 m^3 (375 MW(TH)) and for the 1 GW(E) configuration (250 MW(E)/reactor), the effective volume requirement was calculated to be 117.5 m^3 (470 MW(TH)). Also, sizing an HTR without a complete reactor design implies extrapolating geometrical ratios of an already existing HTR into the dimensions required for the PBMR of the present study. These geometrical ratios were obtained from a Chinese HTR test reactor producing 10 MW(TH) [26]. Installing a high power density nuclear plant in a submarine requires redesigning the traditional reactor geometry in order to suit the internal hull cylinder shape. This was done by modifying the effective volume diameter to height ratio, commonly reaching ratios of 2:1. This process relies on iteration loops until the ratio maximises the space between reactor and internal hull shell. Three effective volume diameter to height ratio (h/D) configurations were tested in AutoCAD, 1/1, 0.8/1 and 0.6/1 so as to determine the optimum geometrical ratio. Table 7 shows the effective volume diameter and height requirement for each thermal power output and effective volume ratio.

Table 7. Effective volume height and diameter values vs thermal outputs.

h/D	280 MW(TH)	375 MW(TH)	470 MW(TH)
1/1	h = 4.47 m/D = 4.47 m	h = 5 m/D = 5 m	h = 5.3 m/D = 5.3 m
0.8/1	h = 3.8 m/D = 4.78 m	h = 4.24 m/D = 5.3 m	h = 4.58 m/D = 5.7 m
0.6/1	h = 3.16 m/D = 5.26 m	h = 3.5 m/D = 5.84 m	h = 3.77 m/D = 6.3 m

Figure 7 represents the contour of the reactor for 3 different thermal output values of 280 MW(TH), 375 MW(TH) and 470 MW(TH) for constant effective volume height to diameter ratio values. This exercise yields very approximate dimensions that do not include balance of plant components. These will increase the dimension of the reactor, in particular the height of the reactor. Height is the critical dimension in the present design. This exercise gave results that are compatible with current experience, but do not include the significant balance-of-plant components required to operate and control the reactor. To the height evaluated here, an arbitrary balance of plant factor was added to give a total operational reactor height of 16–17 m.

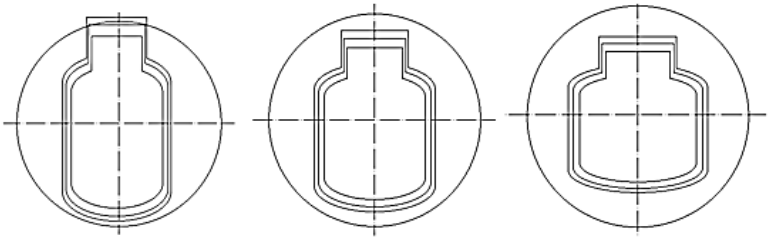

Figure 7. 1/1, 0.8/1 and 0.6/1 Effective volume height to diameter ratio.

5.7. Nuclear Reactor Shielding and Reactor Power Output Selection

To determine the maximum reactor size and thermal output, reactor shielding material thickness had to be calculated as a function of the material used and the required radioactive attenuation depending on the radioactive levels in the reactor vessel proximities and the allowed radiation level for a nuclear plant worker. Material shielding effectiveness is reflected in a linear attenuation coefficient, offering higher levels of attenuation for higher coefficient values. The mass absorption coefficient appears similar for most shielding materials, showing a more noticeable stratification for high gamma energy values. Lead offers the highest value for the whole gamma energy spectrum [19]. Higher density materials such as tungsten offer higher linear attenuation coefficients, since it is the product of mass attenuation coefficient and material density. Lead and Tungsten reactor shield thickness values were obtained and compared. In a preliminary analysis, tungsten offers top-of-line specifications and shows the lowest thickness value from this range of materials (Table 8). However, lead offers a mass attenuation coefficient that could keep up with tungsten at a much lower price and better machining properties. Material melting point was taken into account, as the reactor would operate at 1100 K and lead melting point is 600 K. The 500 K temperature difference should be reduced by cooling. Lead appears as the most economical option for reactor shielding and tungsten outstands in performance but lacks in machining capabilities at a higher price.

Table 8. Shielding properties for different materials [19].

Material	Density [g/cm^3] (20 °C)	Melting Point [K]	HVL [cm]
Aluminium	2.7	973	6.8
Iron	7.86	1808	2.2
Bismuth	9.8	544	1.4
Lead	11.34	600	1.2
Tungsten	19.3	3683	0.8

The required shielding material thickness depends on the radiation attenuation required and the shielding material linear attenuation coefficient. Linear attenuation coefficients are difficult to obtain from public data and so the reactor shielding equation can be modified as follows.

$$\dot{X} = \dot{X}_o \cdot e^{-\mu \cdot \rho \cdot x} \tag{11}$$

Limitation of radiation dose for radiation workers is delimited to 20 mSv/year, according to the International Commission on Radiological Protection [27] and shield thickness is given as follows:

$$x = -\frac{1}{u} \cdot \ln\left(\frac{\dot{X}}{\dot{X}_o}\right) \tag{12}$$

No public data was found for radiation exposure rates emitted per UO2 mass unit in the core. However, the reactor shielding thickness could not restrict the nuclear reactor sizing as the layer of lead or tungsten could be implanted outside the vessel internal hull, increasing the available space for reactor and auxiliary equipment. Based on the current study considerations, 470MW(TH) thermal output per reactor was selected with a 0.6/1 effective volume height.

5.8. Overall Component Integration and Power Plant G.A.

Once reactor shielding thickness, internal hull mechanical design, reactor sizing and optimum geometrical ratios are calculated, they were integrated into the submersible vessel so as to fulfill it's power plant design criteria. The overall design criteria relied on space availability, installing the highest electrical power output, costs, complexity and safety

features. Considering all these, the following reactor and turbomachinery arrangement was proposed.

To achieve weight balance neutrality, the reactors were positioned in the vessel center and isolated by radiation shield. The 4 independent internal hulls offer extra isolation in case of radioactive leak. An extra pressure hull towards the vessel stern is required for accommodating the waterjet propulsion system. This space would house the electrical motors driving the axial-flow impellers and the propulsion auxiliary systems. Figure 8 shows an approximate arrangement. It is considered that there is sufficient length and width to fit the reactors and generating equipment in this hull. However, given the large uncertainty of the height of the reactor, a conning tower of a width similar to the width of the hull and a height similar to the conning tower of the Typhoon-class will be needed to accommodate balance of plant equipment. This is an area that will be explored. This conning tower will provide space for reactor services such as pebble handling and short term storage. The conning tower will also provide space for crew and navigation needs. It is anticipated that the crew of this submersible will be very small given that most of the time it will be stationary producing electricity onshore. Any emergency sailings will be of a very short duration, less than a day. Longer journeys to the maintenance base in the UK would be very infrequent and last very few days. It is also expected that extensive automation will be implemented.

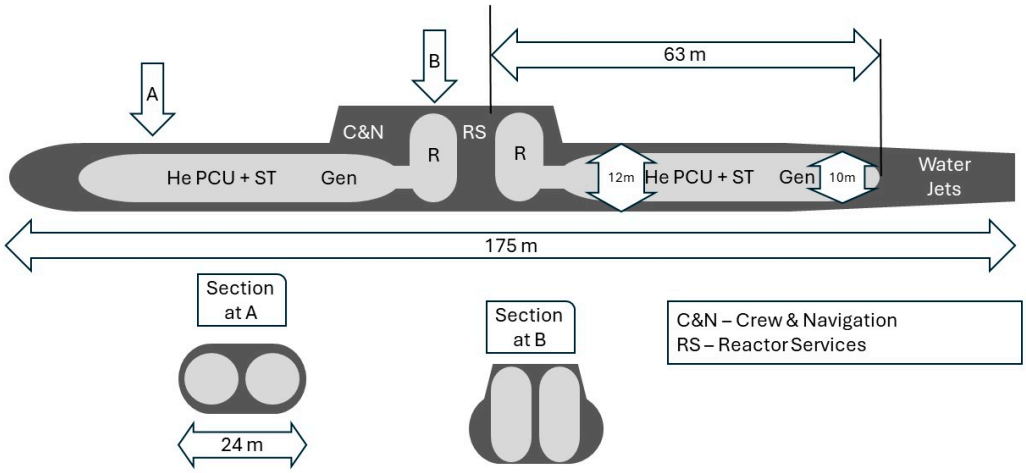

Figure 8. Submersible power plant general arrangement.

The compressor, turbines and generator were arranged in a single shaft towards the bow and the stern of the vessel for weight balance neutrality. This also ensures a safe reactor shutdown, by transferring the torque being delivered to the generator to the shaft, increasing shaft speed and ensuring that the decay heat produced after shutdown is removed. The generator would be situated between the helium and steam turbines [28], in case the steam turbine needs to be disconnected for start-up or maintenance (Figure 9).

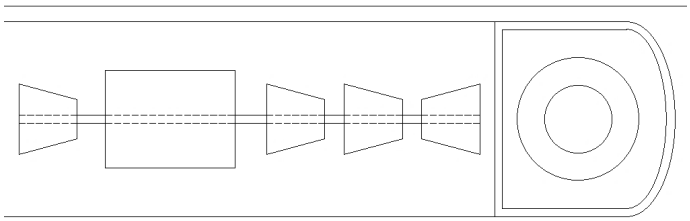

Figure 9. Single shafted turbomachinery and reactor arrangement.

The four internal pressure hull design had advantages over the two pressure hull one, reducing the required internal pressure hull thickness in 20 mm and the system total weight in 8.8%. This weight reduction implies saving 1186 m^3 of ballast tank. In case of

radiation leak in any reactor, the 4 pressure hull design could provide isolation for the rest of reactors. Regarding reactor sizing, the area of largest current uncertainty for this concept, different effective volume height to diameter ratios were analysed so as to install the maximum possible thermal output per unit. In a preliminary analysis, the reactor shielding thickness could restrict the maximum power output per reactor. Integrating the shielding material outside the internal hull would provide more space in the hull to install a larger reactor. This is expected to require the provision of the aforementioned conning tower. Turbomachinery space availability evaluation was also carried out to ensure that total length and diameter of these machines is not a restricting factor. None of the turbomachinery analysed showed total diameters above 2.5 m, leaving enough space for auxiliary equipment and piping.

6. Conclusions

A preliminary view of a submersible nuclear power plant is proposed aimed at delivering zero carbon electricity. This concept greatly reduces the perception of risk associated with nuclear power. The concept is tsunami, earthquake and proliferation proof.

The focus of this study is primarily on the power conversion unit and how to fit in in the envelope of an existing hull, noting that this will be a new submersible and not a retrofit. In the present study the authors, in this first attempt, adhered rigidly to the envelope size of the existing submersible, where the public information available was used as an input for the analysis. This may need to be modified once a second step is carried out on a more detailed analysis of the reactor at the core of the concept. Reactor shape and size constraints are recognised and not dealt in detail here. Extensive additional analysis will be needed on the assessment of the reactor shape and size and the redesign of the submersible shape to accommodate operational and safety requirements. There is some flexibility in altering the shape of the envelope of the submersible, considering that a maximum operating depth of 70–100 m will be adequate. The original test depth of the Typhoon-class was a much deeper 400 m [11]. This large reduction of operating depth and pressure will significantly reduce the constraints on hull design and permit alternative shapes in the vicinity of the reactors to accommodate their requirements. The authors consider the results described here as an encouragement to progress to the next stage, as described in this paragraph. The authors believe that there will be many rewards arising form a more detailed evaluation.

What is presented here is the first iteration in what could be a very long design process. This first iteration has many estimations, uncertainties and methods are used that are considered generic. Nonetheless the outcome is a favourable one and the main conclusion is that the concept appears to be a promising one and further evaluations, refinements and optimisations are recommended.

In a some additional topic of investigation are helium leakages, neutronic coupling between cores and reactor control. Whole system control is going to be very important during an emergency decoupling.

Author Contributions: Conceptualization, P.P.; methodology, J.S., P.P. and E.A.P.; software, D.F., J.S. and P.P.; formal analysis, J.S., P.P. and D.F.; investigation, J.S., E.A.P., S.R., D.F. and P.P.; data curation, J.S., E.A.P., S.R., D.F. and P.P.; writing, D.F., J.S. and P.P.; visualization, P.P.; supervision, P.P. All authors have read and agreed to the published version of the manuscript.

Funding: This research received no external funding.

Institutional Review Board Statement: Not applicable.

Informed Consent Statement: Not applicable.

Data Availability Statement: Data are contained within the article.

Conflicts of Interest: The authors declare no conflict of interest.

Nomenclature

ASME	American Society of Mechanical Engineers
C_p	Specific Heat at constant pressure [J/(Kg·K)]
GT-MHR	Gas-Turbine Modular Helium Reactor
HRSG	Heat Recovery Steam Generator
HVL	Half Value Layer
η_{poly}	Polytropic efficiency [-]
$\dot{m}$	Mass flow rate (kg/s)
OPR	Overall Pressure Ratio
P	Pressure [Pa]
PBMR	Pebble Bed Modular Reactor
PT	Power Turbine
PWR	Pressurized Water Reactor
PR	Pressure Ratio
Q	Thermal output (MW)
RBMK	Reaktor Bolshoy Moshchnosti Kanalnyy
RHR	Residual Heat Removal
SF	Safety Factor
ST	Steam Turbine
T	Temperature [K]
TET	Turbine Entry Temperature
TL	Tangential Line
u	Linear attenuation coefficient [cm^{-1}]
x	Thickness [cm]
$\dot{X}$	Radiation exposure rate (with the shield in place) [Sv/s]
$\dot{X}o$	Exposure rate without the shield [Sv/s]
μ	Mass absorption coefficient

References

1. Andrews, R. Emissions Reductions and World Energy Demand Growth. 2016. Available online: http://euanmearns.com/emissions-reductions-and-world-energy-demand-growth/ (accessed on 14 April 2020).
2. World Nuclear Association. How Can Nuclear Combat Climate Change? 2020. Available online: https://www.world-nuclear.org/nuclear-essentials/how-can-nuclear-combat-climate-change.aspx (accessed on 15 January 2020).
3. Partanen, R. The Most Dangerous Nuclear Power Plant, Energy Reporters. 2018. Available online: https://www.energy-reporters.com/opinion/the-most-dangerous-nuclear-power-plant/ (accessed on 16 January 2020).
4. Rawesat, A.; Pilidis, P. 'Greening' an Oil Exporting Country: A Hydrogen and Helium Closed-cycle Gas Turbines Case Study. *Clean Energy Sustain.* **2024**, *2*, 10005. [CrossRef]
5. Electrek. UK Could Accelerate Its All-Electric Car Plan, Move Target to 2030 or 2035. 2019. Available online: https://electrek.co/2019/05/01/uk-electric-cars-2030/ (accessed on 13 July 2020).
6. Mourouzidis, C.; Singh, G.; Sun, X.; Huete, J.; Nalianda, D.; Nikolaidis, T.; Sethi, V.; Rolt, A.; Goodger, E.; Pilidis, P. Abating CO2 and non-CO2 emissions with hydrogen propulsion. *Aeronaut. J.* **2024**, *128*, 1–18. [CrossRef]
7. Pilidis, P.; Igie, U.; Sethi, V.; Sampath, S.; Nikolaidis, T. Greening A Country: UK Energy Use and Considerations. Technical Paper 652. *The Power Engineer*, June 2023.
8. World Nuclear Association. Chernobyl Accident 1986. 2020. Available online: https://www.world-nuclear.org/information-library/safety-and-security/safety-of-plants/chernobyl-accident.aspx (accessed on 15 April 2020).
9. World Nuclear Association. Fukushima Daiichi Accident. 2020. Available online: https://www.world-nuclear.org/information-library/safety-and-security/safety-of-plants/fukushima-daiichi-accident.aspx (accessed on 18 April 2020).
10. Pletcher, J.P.; Rafferty, K. Japan Earthquake and Tsunami of 2011. 2020. Available online: https://www.britannica.com/event/Japan-earthquake-and-tsunami-of-2011 (accessed on 16 April 2020).
11. Wikipedia. Typhoon-Class Submarine. 2024. Available online: https://en.wikipedia.org/wiki/Typhoon-class_submarine (accessed on 25 October 2024).
12. Phillips, K.E. Helium Gas Turbines for Nuclear Power. Ph.D. Thesis, California US Naval Postgraduate School, Monterey, CA, USA, 1956.
13. Office of Satellite and Product Operations. Sea Surface Temperature (SST) Contour Charts. 2019. Available online: https://www.ospo.noaa.gov/Products/ocean/sst/contour/ (accessed on 26 June 2020).
14. McDonald, C.F. *Helium Turbomachiime Design for GT-MHR Power Plant*; General Atomics: San Diego, CA, USA, 1994; p. 14.
15. SNETP—The Sustainable Nuclear Energy Technology Platform. HTR Information Reference Document Deliverable D12, p. 78. 2009. Available online: www.europairs.eu (accessed on 14 April 2020).

16. SSBN Typhoon Class (Type 941). Naval Technology. 2020. Available online: https://www.naval-technology.com/projects/ssbn-typhoon-class/ (accessed on 14 April 2020).
17. Typhoon Class Submarine Propellers. Available online: https://www.pinterest.es/pin/28217935135386271/ (accessed on 14 April 2020).
18. ASME. ASME VIII Boiler and Pressure Vessel Code. 2017. Available online: https://www.asme.org/getmedia/c041390f-6d23-4bf9-a953-646127cfbd51/asme-bpvc-brochure-webview.pdf (accessed on 23 June 2020).
19. McAlister, D.R. Gamma Ray Attenuation Properties of Common Shielding Materials. *Lane Lisle*, 18 June 2018.
20. Thoughtco. The World's Highest Recorded Temperatures. 2019. Available online: https://www.thoughtco.com/highest-temperature-ever-recorded-1435172 (accessed on 14 April 2020).
21. Materials, A. ASTM A516 Grade 60 and ASME SA516 Grade 60 Carbon Steel Plate Features, Applications and Composition by Masteel. 2009. Available online: https://www.azom.com/article.aspx?ArticleID=4785 (accessed on 14 April 2020).
22. Mueller. 2:1 Elliptical Flanged and Dished Tank Head. 2020. Available online: https://www.paulmueller.com/tank-components/tank-heads/2-1-elliptical-flanged-and-dished-tank-head/ (accessed on 3 July 2020).
23. Heckman, K. Torispherical Head Volume, vCalc. 2020. Available online: https://www.vcalc.com/wiki/vCalc/Torispherical+Head+-+Volume (accessed on 3 July 2020).
24. GE. GE STF-200/100 Steam Turbine Series. 2020. Available online: https://pdf.directindustry.com/pdf/ge-steam-turbines/steam-turbine-stf-200-100-series/116289-943353.html (accessed on 3 July 2020).
25. Idaho National Laboratory. *High Temperature Gas-Cooled Reactor Technology Training Curriculum*; Idaho National Laboratory: Idaho Falls, ID, USA, 2019.
26. Qin, Z. General Design of the 10MW HTR. 2016. Available online: https://www.gen-4.org/gif/upload/docs/application/pdf/2022-12/jaeri_96_010_htr10generaldesign.pdf (accessed on 14 April 2020).
27. Lekchaum, S.; Locharoenrat, K. Calculation of Lead-Iron Double-Layer Thickness for Gamma-Ray Shielding by MATLAB Program. *Hindawi Sci. Technol. Nucl. Install.* **2017**, *2017*, 6078461. [CrossRef]
28. Serna, J. Submersible Nuclear Power Station. MSc Thesis, Cranfield University, Bedford, UK, 2020.